





Article

Two *Nothofagus* Species in Southernmost South America Are Recording Divergent Climate Signals

Pamela Soto-Rogel ^{1,2,3,*}, Juan Carlos Aravena ^{2,3,†}, Ricardo Villalba ⁴, Christian Bringas ², Wolfgang Jens-Henrik Meier ¹, Álvaro Gonzalez-Reyes ^{5,6} and Jussi Grießinger ^{1,†}

- ¹ Institute of Geography, Friedrich-Alexander-Universität Erlangen-Nürnberg, 91058 Erlangen, Germany; wolfgang.jh.meier@fau.de (W.J.-H.M.); jussi.griessinger@fau.de (J.G.)
- ² Centro de Investigación GAIA Antártica, University of Magallanes (UMAG), Punta Arenas 6200000, Chile; juan.aravenadonaire@gmail.com (J.C.A.); chbr.skt@gmail.com (C.B.)
- ³ Cape Horn International Center (CHIC), Puerto Williams 6350000, Chile
- ⁴ Instituto Argentino de Nivología, Glaciología y Ciencias Ambientales (IANIGLA-CONICET), Mendoza 5500, Argentina; ricardo@mendoza-conicet.gob.ar
- ⁵ Hémera Centro de Observación de la Tierra, Escuela de Ingeniería Forestal, Facultad de Ciencias, Universidad Mayor, Huechuraba 8580745, Chile; gonzalezreyesalvaro@gmail.com
- ⁶ Centro FONDAF de Investigación en Dinámica de Ecosistemas Marinos de Altas Latitudes (IDEAL), Valdivia 5090000, Chile
- * Correspondence: pamelasoto.rogel@fau.de
- † These authors contributed equally to this work.

Abstract: Recent climatic trends, such as warming temperatures, decrease in rainfall, and extreme weather events (e.g., heatwaves), are negatively affecting the performance of forests. In northern Patagonia, such conditions have caused tree growth reduction, crown dieback, and massive dieback events. However, studies looking at these consequences in the southernmost temperate forest (*Nothofagus betuloides* and *Nothofagus pumilio*) are much scarcer, especially in southernmost South America (SSA). These forests are also under the influence of the positive phase of Antarctic Oscillation (AAO, also known as Southern Annular Mode, SAM) that has been associated with increasing trends in temperature, drought, and extreme events in the last decades. This study evaluated the growth patterns and the climatic response of eight new tree-ring chronologies from *Nothofagus* species located at the upper treeline along different environmental gradients in three study areas: Punta Arenas, Yendegaia National Park, and Navarino Island in SSA. The main modes of the ring-width index (RWI) variation were studied using principal component analysis (PCA). We found that PC1 has the higher loadings for sites with precipitation values over 600 mm/yr, PC2 with *N. betuloides* sites, and PC3 with higher loadings for sites with precipitation values below 600 mm/yr. Our best growth-climate relationships are between *N. betuloides* and AAO and the most northeastern site of *N. pumilio* with relative humidity (which coincides with heatwaves and extreme drought). The climatic signals imprinted in the southernmost forests are sensitive to climatic variability, the climate forcing AAO, and the effects of climate change in the last decades.

Keywords: ring-width index; climate; Antarctic Oscillation (AAO); *Nothofagus betuloides*; *Nothofagus pumilio*



Citation: Soto-Rogel, P.; Aravena, J.C.; Villalba, R.; Bringas, C.; Meier, W.J.-H.; Gonzalez-Reyes, A.; Grießinger, J. Two *Nothofagus* Species in Southernmost South America Are Recording Divergent Climate Signals. *Forests* **2022**, *13*, 794. <https://doi.org/10.3390/f13050794>

Academic Editor: Rafal Podlaski

Received: 25 March 2022

Accepted: 17 May 2022

Published: 19 May 2022

Publisher's Note: MDPI stays neutral with regard to jurisdictional claims in published maps and institutional affiliations.



Copyright: © 2022 by the authors. Licensee MDPI, Basel, Switzerland. This article is an open access article distributed under the terms and conditions of the Creative Commons Attribution (CC BY) license (<https://creativecommons.org/licenses/by/4.0/>).

1. Introduction

Recent climatic trends, droughts, warm temperatures, and extreme events (e.g., heatwaves) have globally affected forest ecosystems causing climate-induced feedbacks, such as growth decline, forest dieback, and even massive tree mortality events [1–7]. According to recent climate projections for upcoming decades, an increase in the severity of droughts, a warmer climate, and an accelerated frequency of extreme events are predicted globally [8].

Droughts and warmer temperatures, for example, result in a negative physiological impact on forest ecosystems in terms of limiting growth, favoring transpiration, and inducing stomatal closure [9]. The temperate forests of South America are already prone to such negative effects caused by drought events and warmer temperatures. For example, dendroecological studies in northern Patagonia revealed that several *Nothofagus* species and coniferous species (*Austrocedrus chilensis*) exhibited episodes of mortality, growth reduction, crown dieback, and extreme depression in response to persistent drought and/or extreme heatwave events during the growing season [10–17]. Physiologically, the forests of northern Patagonia are increasingly under water stress and are therefore showing an adjustment of stomatal conductance to avoid an increasing water shortage. Consequently, their photosynthetic rate decreases, resulting in a lowered basal area increment (BAI). On the other hand, trees growing in better water availability reveal a higher growth performance with current climatic conditions [17–19].

In southernmost South America (SSA), *Nothofagus pumilio* and *Nothofagus betuloides* are the dominant tree species in temperate forests [20,21] and are the main tree species used for monitoring the climate variability and effects of regional climate change. In southern Patagonia, *N. pumilio* stands growing at lower altitude (xeric forest-steppe ecotone) showed a negative tree growth trend in response to a reduction in stomatal conductance induced by the decrease in soil moisture in warmer and drier summers. In contrast, the investigated *N. pumilio* stands at the upper tree line (more humid conditions), indicating more favorable conditions for tree growth benefitting from increasing temperatures during the growing season [22]. The *N. betuloides* forests in eastern Tierra del Fuego (ecotone steppe forest conditions, 54° S, 600 mm/yr) indicate an abrupt decrease in tree growth that can be associated with the predominantly positive summer AAO since the late 1980s [23,24]. On the other hand, the growth of *N. betuloides* in the more humid areas of Tierra del Fuego does not reveal such a marked decrease [25,26].

The Antarctic Oscillation (AAO, also known as Southern Annular Mode, SAM) is a large-scale circulation pattern affecting the climate of large parts of South America. Since the late 1980s, it has revealed a predominantly positive phase during the austral summer [27]. This phase is characterized by positive pressure anomalies at mid-latitudes (40–55° S) and negative anomalies at high latitudes (Antarctica). In the central-eastern sector of SSA, the positive AAO values are associated with ongoing climatic trends, decrease in precipitation, warm temperatures, prevailing drought conditions [28–30], and extreme events (e.g., heatwaves) [31]. Under these recent climatic trends in SSA, few studies have investigated whether the forests of *N. betuloides* and *N. pumilio* respond to climate change-induced effects and how droughts and extreme events (e.g., heatwaves) might affect their growth [11,13–15]. Naturally, the *Nothofagus* forests in SSA represent a promising potential to analyze their response to a changing climate, e.g., by studies on growth reduction and/or extreme events in growth variations. Given the strong ecoclimatic gradient in SSA from a western hyper-humid zone to the dry steppe landscapes in the East (Figure 1). Previous studies revealed that the South American *Nothofagus* forests reveals diverse responses most likely associated with microsite conditions, water availability [22,25,26,32], and species-specific drought adaptation [33].

In this context, our aims are (1) to compare the growth patterns and (2) to individually evaluate climatic responses of *N. betuloides* and *N. pumilio* forest in SSA, including different ecological requirements and under accelerated climate change in the last decades. We hypothesize that the tree's growth of the *Nothofagus* species are sensitive to local and large-scale climatic variations and therefore reveals imprints of short- and long-term climatic variations in the last centuries.

2. Materials and Methods

2.1. Climatic Condition in Southernmost South America

The mountain ranges of the Andes act as marked orographic barriers to westerly winds. The ascent of moisture-laden masses from the Pacific Ocean results in increased

cloudiness and precipitation on the western windward side (reaching up to 5000 mm/yr in some sectors) [34], which decreases markedly on the eastern leeward side with very low rainfall (200 mm/yr) only 50–100 km east of the Cordillera [29]. Climate diagrams of weather stations at Schiaparelli Glacier (163 m asl), Punta Arenas (36 m asl), and Río Gallegos (13 m asl), located along a transect from southwest to northeast in the region, show different monthly mean values in precipitation, air temperature, and relative humidity between stations (Figure 1E–G); while the annual mean temperatures reveal a clear winter–summer seasonality for the three stations, the colder temperatures, higher precipitation, and higher relative humidity at Schiaparelli Glacier may be associated with the strong west–east climatic gradient mentioned above. The Schiaparelli weather station records the highest relative humidity ($rH = 80\%$) distributed homogeneously throughout the year. In contrast, the climatic stations downwind of the Cordillera, such as Punta Arenas and Río Gallegos, only have high rH values during the winter, with a decrease of around 60% and 50% in summer, respectively. Precipitation varies strongly among the three weather stations, with the highest monthly records at Schiaparelli (50–70 mm), intermediate at Punta Arenas (30–40 mm), and the lowest at the Río Gallegos station (15–30 mm).

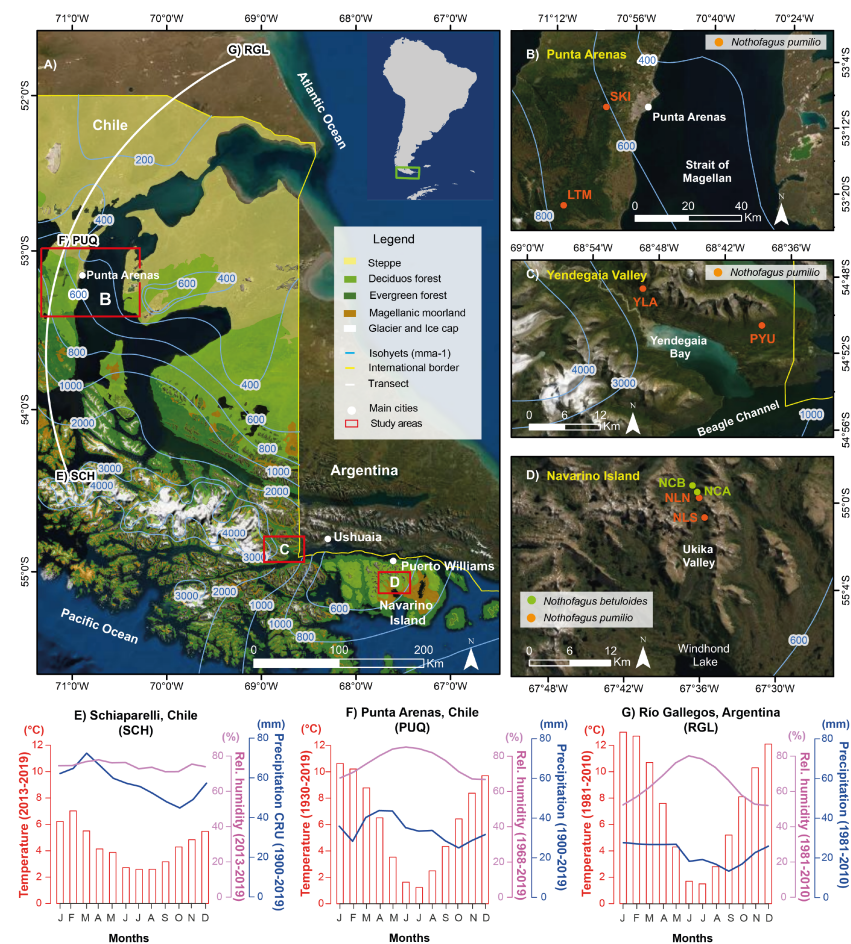


Figure 1. The geographical and climatic setting of the study area. (A) Location of the major towns of Punta Arenas, Ushuaia, and Puerto Williams (white circles) and overview of the three study areas (red boxes): (B) Punta Arenas outskirts ($53^{\circ}9'36''$ S, $71^{\circ}1'54''$ W), (C) Yendegai Valley ($54^{\circ}50'17''$ S, $68^{\circ}45'17''$ W) and (D) Navarino Island ($54^{\circ}58'50''$ S, $67^{\circ}36'23''$ W). Illustration of regional vegetation types [20,35]. The isohyets, glaciers, and political limits are derived from the state-owned geospatial data network IDE (<https://www.ide.cl/>, accessed on 1 May 2022). (E–G) Climate diagrams of three weather stations along a southwest to northeast transect (white line in A), including monthly mean temperature ($^{\circ}$ C), relative humidity (%), and precipitation (mm). The map was created using Esri ArcGIS.

2.2. Tree-Ring Sample from Southernmost South America

Our tree-ring network study encompasses several sites in the southernmost part of South America, including sites at Tierra del Fuego Island and adjacent archipelagos (Figure 1A, Table 1). The strong hydroclimatic gradient determines a rapid variation in biotic communities ranging from hyper-humid to dry environments from the Magellanic moorland and evergreen forests dominated by *N. betuloides*, through deciduous forests dominated by *N. antarctica* and *N. pumilio*, to treeless steppe grasslands [20]. Our eight study sites are located in *Nothofagus* forests, six of the sampling sites are dominated by *N. pumilio* (Lenga), while the remaining two sites consist mainly of *N. betuloides* trees (Coigue de Magallanes). All sampled trees reach grow at elevations above 250 m asl, close to the upper treeline (Figure 1, Table 1). Therefore, our choice of the site locations follows the general requirements to optimize the climatic signal inherent to trees growing near their upper distribution limit [24]. Fieldwork at the eight sites was conducted during the austral summers between 2019 and 2021. Trees were sampled at breast height using 5 mm diameter borers (two samples per tree) in the three selected geographic regions.

Table 1. Sampling-sites main characteristics. Np = *N. pumilio*; Nb = *N. betuloides*. sp* = Species.

Site Code	sp*	Lat (S) Long (W)	Elevation m asl	Timespan AD Years	Number of Trees (Radii)	Trees (Radii) in Chronology	EPS (>0.85) Start.Year
Punta Arenas area							
SKI	Np	53°9'36" 71°1'54"	550	1851–2019	29/(58)	26 (49)	1895
LTM	Np	53°18'59" 71°16'48"	558	1834–2020	32/(64)	27 (40)	1896
Yendegaia Valley area							
YLA	Np	54°48'35" 68°48'35"	566	1764–2019	33/(66)	31 (61)	1770
PYU	Np	54°50'30" 68°38'39"	423	1768–2019	22/(44)	21 (35)	1770
Navarino Island area							
NLS	Np	55°00'38" 67°36'35"	450	1769–2019	20/(40)	20 (32)	1820
NLN	Np	54°59'45" 67°36'00"	403	1852–2019	21/(42)	21 (41)	1870
NCA	Nb	54°59'29" 67°36'9"	350	1699–2019	21/(42)	20 (30)	1870
NCB	Nb	54°59'1" 67°36'32"	275	1739–2019	21/(42)	19 (32)	1845

Close to the city of Punta Arenas (Figure 1B), we sampled two *N. pumilio* forests. The SKI site is located at 550 m asl., 7 km west of Punta Arenas in the forest-to-steppe ecotone. The forests is formed by trees reaching 8–12 m high with an average diameter at breast height (dbh) of 25 cm. Annual rainfall at SKI amounts to 470 mm/yr and is part of the forest-to-steppe. The Lenga Tres Morros site (LTM) is located at an elevation of 558 m asl. It is situated around 40 km southwest of Punta Arenas in a mixed landscape of *N. pumilio* and *N. betuloides* forests with lakes and peatlands (Figure 1B). The LTM stand includes *N. pumilio* individuals with an average tree height of 15 m and a mean dbh of 30 cm, and annual rainfall accounts for 800 mm/yr.

Our second study region is located in the Yendegaia valley at National Park on the southern border of Tierra del Fuego Island (Figure 1C). Rainfall amounts in Yendegaia Bay account for 350 mm/yr, increasing to the upper glacierized areas to 2000–5000 mm/yr.

In total, two high elevation sites with *N. pumilio* forests were sampled. The Yendegaia Lenga Alta site (YLA) is located at an elevation of 560 m asl. Local trees reach average heights between 10 and 15 m and have mean diameters at a breast height of 30 cm. The tree stand is close to a krummholz zone that forms the local upper treeline. The Paso Yendegaia-Ushuaia site (PYU) is located at elevations of around 500 m. Sampled trees are reaching heights of 15–20 m with average dbh values of 50 cm.

The third sample region, the Ukika valley on Navarino Island (Chile), is located in the southeastern part of our study region (Figure 1D). Typically, patches of *N. pumilio* and *N. betuloides* forests are forming the local tree communities in the valley. Annual rainfall amounts 600 mm/yr. We sampled four sites in close proximity to each other. Two sites are dominated by *N. betuloides* forests, namely Navarino Coigue Alto site (NCA) at 350 m asl and Navarino Coigue Bajo (NCB) at 275 m asl. and two sites with *N. pumilio* trees denominated Navarino Lenga Sur (NLS) at 450 m asl and Navarino Lenga Norte site (NLN) at 403 m asl. The site NLS represents the only site in our study located south of the divide separating the north-facing Ukika river watershed from the south-facing Windhond Lake watershed. All sampled sites are characterized by trees of 15–20 m height and dbh of 30–50 cm.

2.3. Samples Preparation and Chronology Building

All tree-ring samples were prepared following standard dendrochronological techniques [36] and considering the tree-ring dating convention for the Southern Hemisphere [37]. Subsequently, tree-ring widths of each sample were measured using a Velmex micrometer with a precision of 0.001 mm [38]. The quality of cross-dating and possible errors in the assignment of calendar ages of the ring widths were evaluated using the COFECHA program [39]. We developed standard tree-ring chronologies from correctly cross-dating series, using the dplR package [40] in the statistical language R [41]. To preserve the low-frequency variations, the ring-width series were detrended using a negative exponential curve to remove non-climatic variability due to the tree's age and obtain the final ring-width index (RWI) [42]. The resulting standardized series represents a mean equal to one and a relatively homogeneous variance over the years [42]. The Expressed Population Signal (EPS) was calculated in a moving window of 50 years with an overlap of 25 years to evaluate the common signal for the chronologies [40,43].

2.4. Principal Component and Regime Shift Analyses

To identify the dominant growth patterns among all sites, we performed a principal component analysis (PCA) using varimax optimization [44,45]. The PCA was performed in the R project [41] using the psych package [46]. The data matrix used included a total number of eight items (standard tree-ring chronologies sites) and n variables (n = number of years used for the analysis), with a time span of 124 years, truncated by the common period of all available chronologies with an EPS above 0.85 (1895 to 2019). Additionally, we explored possible regime shifts in the patterns of the tree-ring chronologies and the principal components time series by the change point detection method [47]. This approach uses the Student's t -test sequentially to determine whether the means between two consecutive periods are significantly different. If this is the case, the point is marked as a potential change point, and subsequent observations are utilized to confirm or disprove the supposed regime shift. The determination of the regimes is strongly influenced by choice of the cut-off length "1", this factor finally defines the length of a regime's minimum period and subsequently the level of significance resulting from the t -test ($p < 0.05$) [47].

2.5. Climate Data

To evaluate climate-proxy relationships, we used two different sources of climate data. The first source are available weather stations close to the respective study sites, such as Puerto Williams (ptw), Punta Arenas1 (puq1), Punta Arenas2 (puq2), and Ushuaia (ush) (Figure 1). The available weather data include various climate parameters, such

as total monthly precipitation (pre: mm), minimum/maximum monthly temperature (tmn/tmx: °C), and wind speed (ws: kmh⁻¹). As the SSA weather stations are (i) short, (ii) with sometimes significant amounts of data gaps, and (iii) elevation differences between the study sites and the nearby climate station. To overcome these obstacles apparent in our study region, we, therefore, decided to use ERA5 reanalysis [48] as a second source of climatic data. ERA5 has a vast variety of climate data with a temporal coverage from 1979 to 2021. It also provides climate data for chosen elevation levels across the area (e.g., at 850 hPa), which enables us to analyze proxy-climate relationships across sites with similar climate influences (Table 2). The ERA5 climate reanalysis datasets [48] additionally provide ancillary eco-climate data, such as monthly means for total precipitation (pre: mm), minimum temperature (tmn: °C), the temperature at 2 m (T2m: °C), 10 m near-surface wind speed (WS10m: m/s), relative humidity (rH: %), the temperature at 850 mb (T850: °C), mean sea level pressure (MSLP: mb), and Geopotential Height (Z850: m²s⁻²) (Table 2). The record from each available meteorological station reveals different temporal coverages and data completeness. For example, climate data from the Puerto Williams weather station are available from 1968 onwards, but with several data gaps during the recording period. For this reason, we used different common periods for the calibration with precipitation (1970–2019) and temperature data (1980–2019) in our analyses. In addition, an abnormal abrupt shift in the mean wind speed is evident around 1984/85 (S1). Given that it was impossible to discern if this abrupt change is induced by instrument/technical changes or climatically caused, we truncated the original full climate data series for wind speed to the reliable period 1986–2019 (Table 2). In contrast, all ERA5 reanalysis data products are available since 1979 until today (Table 2).

Additionally, to evaluate the relationships between the tree-ring chronologies and regional effective large-scale atmospheric circulation patterns, we used two AAO indices commonly used in climatology, namely the AAO-Marshall [27] and the AAO-NCEP index [49]. Those indices differ in the respective climatic variables and data sources used for their calculation. The AAO-Marshall Index is a monthly index available from 1957 to the present. It is calculated by differences in zonal pressures based on 12 meteorological stations, where six of these are located in the mid-latitudes (40° S) and the remaining six in the high latitudes on Antarctica (65° S) [27]. The monthly AAO-NCEP index is based on geopotential height field anomalies at 700 mb height for the Southern Hemisphere and available since 1979 [49].

Table 2. Local climatic records and ERA5 reanalysis data used for the evaluation of proxy-climate relationships. Climate data sources: Dirección Meteorológica de Chile (DMC), Dirección General de Agua Chile (DGA), Servicio Nacional Meteorológico Argentino (SNM), and the ECMWF Reanalysis v5 (ERA5).

Weather Station	Lat (S) Long (W)	Variable	Period	Source
Punta Arenas1 (puq1)	53°0'6" 70°50'50"	pre: precipitation	1900–2019	DMC
		tmn: minimum temperature	1930–2019	
		tmx: maximum temperature	1930–2019	
		ws: wind speed	1967–2019	
Punta Arenas2 (puq2)	53°7'24" 70°52'38"	pre: precipitation tmn: minimum temperature tmx: maximum temperature	1974–2019	DGA
Ushuaia (ush)	54°48'0" 68°18'6"	pre: precipitation tm: mean temperature	1928–2013 1901–2014	SMN

Table 2. Cont.

Weather Station	Lat (S) Long (W)	Variable	Period	Source
Puerto Williams (ptw)	54°55′54″ 67°36′36″	pre: precipitation	1970–2019	DMC
		tmn: minimum temperature	1980–2019	
		tmx: maximum temperature	1980–2019	
		ws: wind speed	1986–2019	
ERA5	Reanalysis	pre: precipitation	1979–2019	[48]
		tmn: minimum temperature		
		T2m: temperature 2 m		
		WS10m: near surface wind speed		
		rH: relative humidity		
	MSLP: Sea Level Pressure			
	MZ850: Geopotential Height 850 mb			

3. Results

3.1. Tree Growth Patterns

In total, we were able to develop eight new tree-ring-width index (RWI) chronologies for southernmost South America (SSA), including two different *Nothofagus* species. The tree-ring chronologies cover different timespans and show differences in growth trends (Figure 2, Table 1). The most extended time series is the *N. betuloides* chronology from Navarino Island (NCA; 1698–2018, 320 years), while the shortest series is the *N. pumilio* chronology from Punta Arenas (SKI; 1851–2019, 169 years). Besides their time spans, the chronologies also differ in sample replication, and consequently, in the period when their EPS values reach or surpass the commonly used threshold of 0.85 [50]; more statistical details can be found in Supplementary Table S1. The *N. pumilio* chronologies SKI, YLA, and PYU reach EPS values above 0.85 with 5 or more cores, the NLS, NLN, and the *N. betuloides* chronology NCB needed around 10 or more cores, while the LTM and NCA records needed almost 20 cores for reaching EPS > 0.85. Differences in the time length of the reliable tree-ring chronologies (EPS > 0.85) reflect variations in the strength of the common signal between sampled tree stands. The chronologies also differ in the amplitude of the tree growth variations. SKI and PYU show the largest amplitudes with marked extreme values. On the contrary, the other six chronologies (LTM, NLS, NLN, NCA, and NCB) show narrower amplitudes. This is especially the case for NLN site, with slight variations in tree-ring widths around the mean (Figure 2E). A regime shift analysis for the eight chronologies [47] reveals marked tree-ring changes but not persistent trends in the records (Figure 2). Only the NLS series chronology shows a gradual progression to more positive values (Figure 2F). Conversely, the *N. betuloides* NCA and NCB chronologies from Navarino Island show a sharp and clear growth decline over the last 40 years, with values beneath the long-term mean since the mid-1980s (Figure 2G,H).

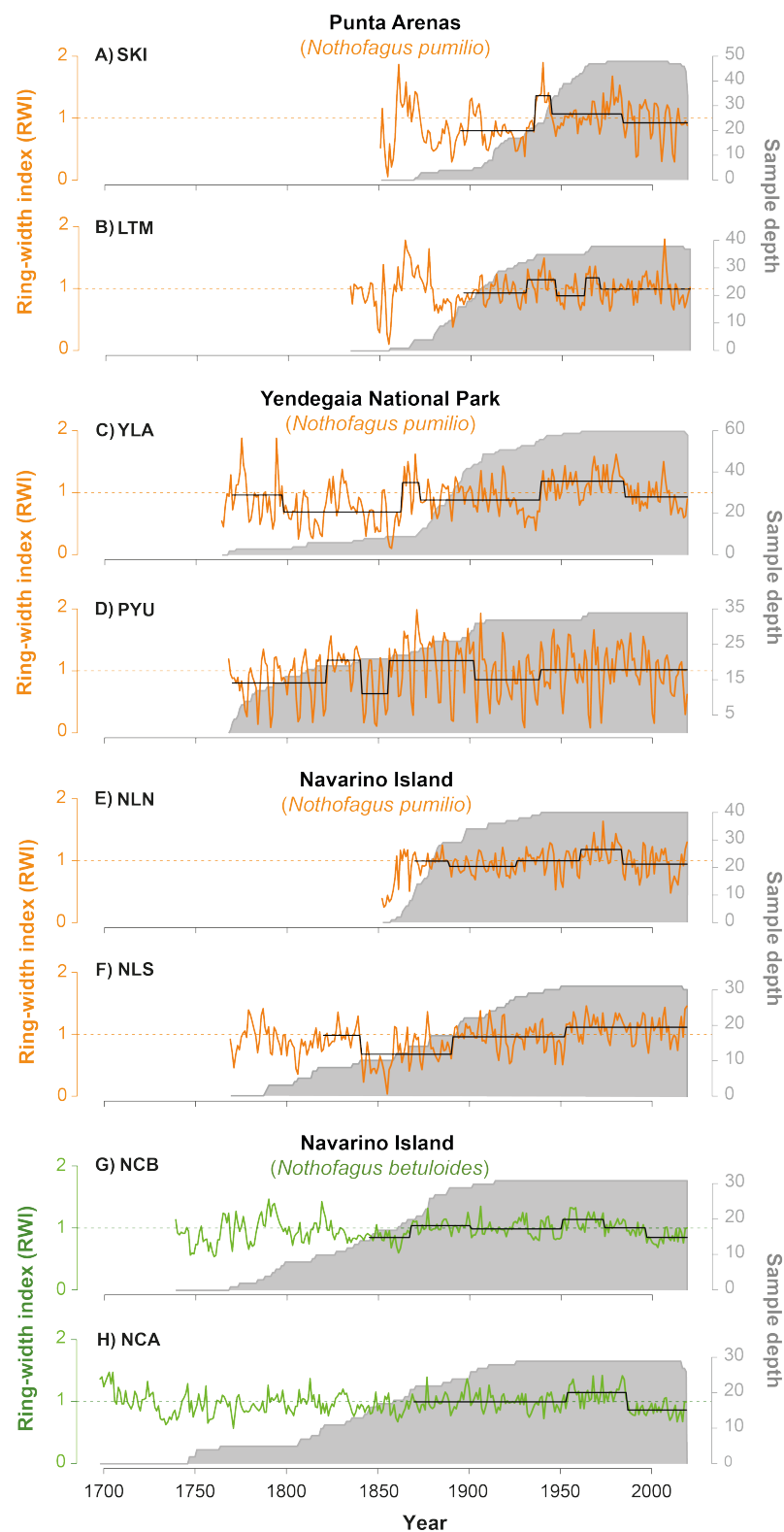


Figure 2. Individual ring-width index (RWI) *N. pumilio* (orange) and *N. betuloides* (green) chronologies are displayed as continuous lines. Horizontal dotted lines indicate mean RWI value, grey shading lines the sample depth, and continuous black lines the regime shifts using the detection method [47]. This regimen shift analysis was calculated for the period with chronology EPS values exceeding the threshold of 0.85 (EPS calculated in a moving window of 50 years with an overlap of 25 years [43]).

3.2. Relationships between the Individual Ring-Width Index Chronologies

Interestingly, despite enormous differences in site conditions, all *Nothofagus* spp. chronologies are positively correlated with each other (Figure 3). Most significant correlations occur between the *N. betuloides* chronologies NCA and NCB ($r = 0.75$, $p < 0.01$) and between the *N. pumilio* NLN and NLS ($r = 0.65$, $p < 0.01$) chronologies in Navarino Island. Although the *N. pumilio* sites (NLN and NLS) and *N. betuloides* sites (NCA and NCB) are geographically located close to each other (2.0 to 0.5 km), they are not significantly related. In contrast to this finding, the NCA and YLA from *N. betuloides* and *N. pumilio*, respectively, separated by more than 80 km are correlated significantly with each other ($r = 0.51$, $p < 0.01$). Positive relationships are also recorded between the sites NLN and LTM (almost 300 km apart, $r = 0.49$, $p < 0.01$), NLN and YLA (more than 80 km apart, $r = 0.47$, $p < 0.01$), and NLS and LTM (300 km apart, $r = 0.45$, $p < 0.01$). Conversely, weaker relationships are apparent between the chronologies from the Punta Arenas area, SKI, and LTM (25 km apart, $r = 0.32$, $p < 0.01$) and from the Yendegaia area, YLA, and PYU (12 km apart, $r = 0.42$, $p < 0.01$).

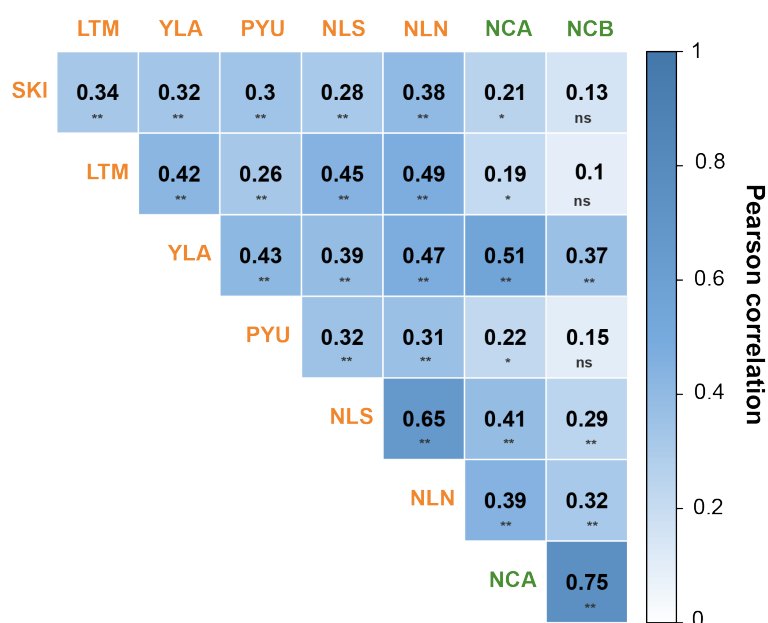


Figure 3. Pearson correlation coefficients between *Nothofagus* standardized ring-width index (RWI) chronologies from sampling locations in SSA over 1895–2019, the interval showing EPS > 0.85 in all records. *N. pumilio* and *N. betuloides* chronologies are shown with orange and green colors, respectively. Levels of significance are illustrated by ns: not significant ($p > 0.05$), *: significant ($p < 0.05$) and **: highly significant ($p < 0.01$).

3.3. Evaluation of Regional Tree Growth Patterns

Regional patterns of tree growth were analyzed by applying a Principal Component Analysis (PCA). Based on the 124-year correlation matrix of the common period among the standardized chronologies, the first three principal components explain 70% of the total variance (Figures 4A and Supplementary Figure S2). PC1, accounting for 44% of the total variance, is mainly associated with the *N. pumilio* chronologies LTM, NLS, and NLN with loading values > 0.5 (Figure 4B). The respective study sites are located in areas with precipitation amounts between 600 and 800 mm/yr. Whereas the NLS and NLN sites are located close to each other (less than 4 km apart), the LTM is more than 400 km away from both sites (Figure 1A,D). The three chronologies agreed in the regime change around 1960 (Figure 2B,E,F). PC2 explains 16.5% of the total variance, and its highest loading values are from the *N. betuloides* chronologies NCA and NCB (Figure 4B). PC2 is clearly dominated by these two close records (less than 2 km apart) with forests having the same species and presenting identical regimen patterns (Figure 2G,H). PC3 only explains 10.5% of the total variance (Figure 4D), highlighting the similar tree growth patterns of the *N.*

pumilio chronologies from the SKI, PYU, and YLA sites (Figure 2A,C,D). These sites have precipitation amounts between 350 and 470 mm/yr, with SKI 400 km north of YLA and PYU (Figure 1A–C).

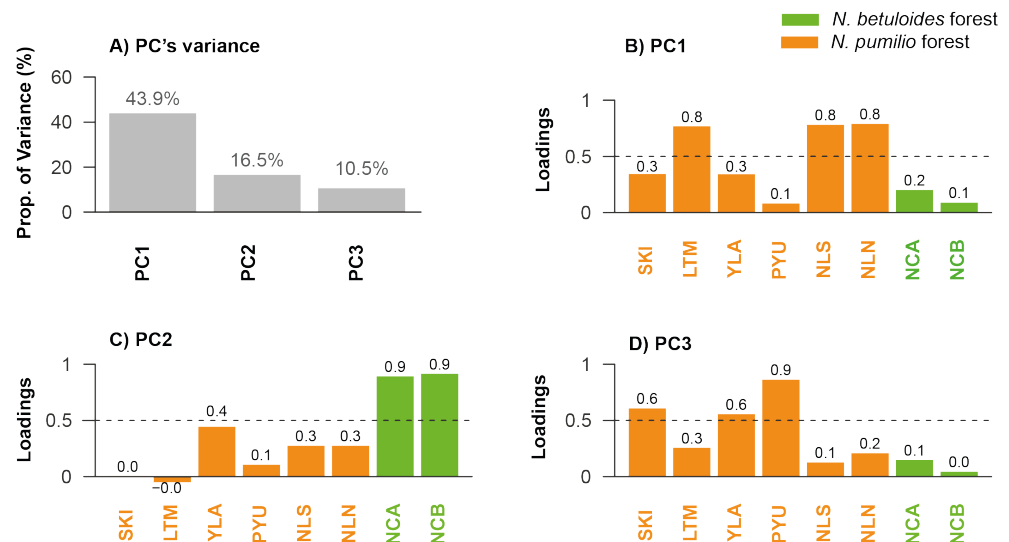


Figure 4. Results of the Principal Component Analysis (PCA) of all eight *Nothofagus* spp. chronologies over the common period 1895–2019. (A) PC variance explained by the first three components (grey boxes). (B–D) Loading values of each site in PC1, PC2, and PC3, respectively.

The resulting principal components PC scores are shown in Figure 5. The PC1 scores (Figure 5A) show a slightly positive trend from 1895 to the present. The PC2 time series (Figure 5B), associated with the *N. betuloides* growth patterns from Navarino Island, shows two regimes shifts to positive in 1951 and negative in 1985, the latter related to an abrupt decline in tree growth. The PC3 scores represent the dominant influence of the *N. pumilio* chronologies with low-loadings in PC1. PC3 varies along with the mean with shifts out of phase with the two previous main modes of tree growth variation (Figure 5C).

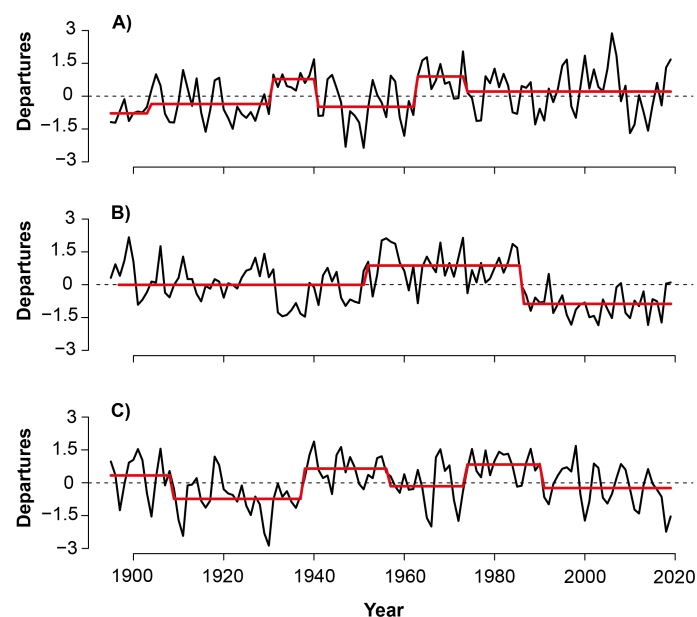


Figure 5. Amplitudes of the principal components PC1 (A), PC2 (B), and PC3 (C) based on the correlation matrix of the standardized chronologies of *Nothofagus* spp. (black lines) for the common period 1895–2019. The red horizontal lines show the regime shifts in the PCs using the detection method [47].

3.4. Influence of Local Climate on the RWI Chronologies

Extreme growth suppressions in the last decades are apparent for the SKI chronology in 1991/1992, 1999/2000, 2005, and 2011/2012 (Figures 2A and 6A). The SKI chronology is positively correlated with ERA5 relative humidity during February of the previous (pF) and current (cF) years (Figure 6A: $r = 0.62$, $p < 0.01$). On the other hand, growth variations in the LTM site are positively correlated with maximum summer temperature during austral summer (current December–January) (Figure 6B: $r = 0.47$, $p < 0.01$). Although the SKI/LTM sites are only 40 km apart, they do not show similar correlation patterns with the local climate (Supplementary Figure S3).

At Yendegaia, the PYU site reveals a highly significant relationship with wind speed of the previous/current summer (January to March) (Figure 6C, $r = 0.62$, $p < 0.01$, Supplementary Figure S4). In contrast, the NLS site on Navarino Island with *N. pumilio* as the dominant tree species reveals an inverse correlation with wind speeds from Puerto Williams for the current year spring/summer transition period (October–November) (Figure 6D, $r = -0.47$, $p < 0.01$, Supplementary Figure S5). Another notable correlation is the NCA site with summer temperatures from ERA5 data (Figure 6E, $r = 0.54$, $p < 0.01$, Supplementary Figure S6).

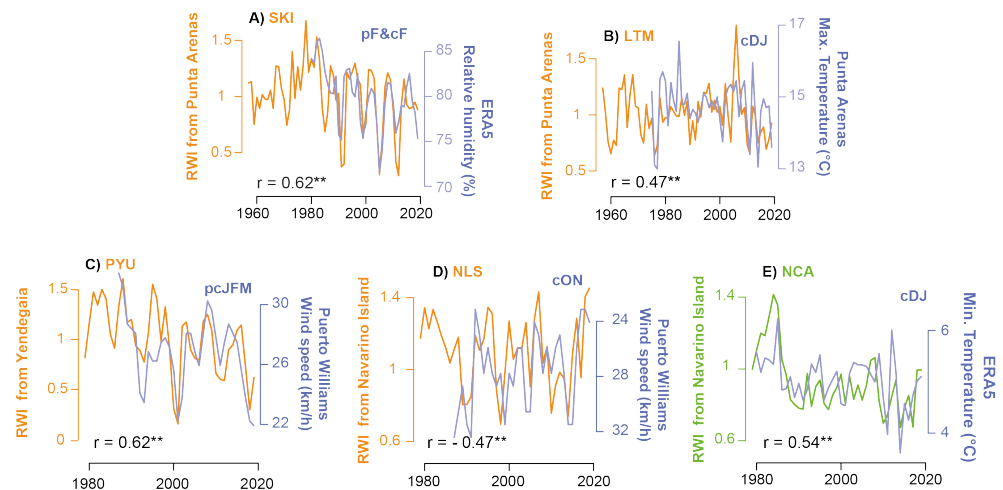


Figure 6. The most significant relationships between ring-width index (RWI) and climate variations at local weather stations and the ERA5 dataset. Significance is indicated for each case: ** = $p < 0.01$. The best combination of months for the climate-growth correlations were: pF&cF = previous and current February, cDJ = current December to January, pcJFM = previous and current January to March and cON = current October to November.

3.5. Influence of Large-Scale Circulation Forcings on the RWI Chronologies

Results for the evaluation of large-scale atmospheric forcings on our series reveal the strongest relationships between our SSA RWI chronologies and different Antarctic Oscillation indices (AAO, also known as Southern Annular Mode, SAM) are mainly negative (Figure 7 and see supplementary material). The Marshall AAO index during the previous/current summer-autumn period is strongly related to the radial growth of the NCB and NCA *N. betuloides* chronologies from Navarino Island (Figure 7C, $r = -0.62$, $p < 0.01$; Figure 7B, $r = -0.53$, $p < 0.01$, respectively). The *N. pumilio* YLA site from Yendegaia shows a good relationship with the AAO-NCEP index from December to May, but is comparably weaker (Figure 7A, $r = -0.48$, $p < 0.01$).

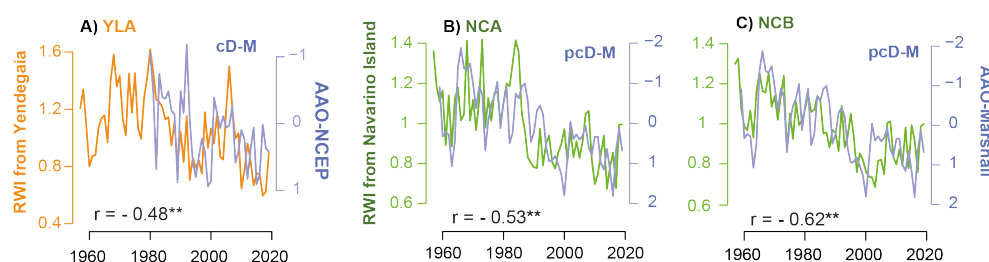


Figure 7. The most significant relationships between the ring-width index (RWI) from SSA and the Antarctic Oscillation (AAO). Significance is indicated by ** = p -value < 0.01. The best combination of months for the climate-growth correlations were: cD-M = current December to May, pcD-M = previous and current December to May.

3.6. Influence of the Local and Large-Scale (AAO) Climate on Principal Components

Consistent with the previous section results, the three dominant patterns of the radial growth, identified by the principal components (PC) analysis, are significantly correlated with local climate and AAO indices (Figure 8 and Supplementary Figure S7). Current March wind speed measured at Puerto Williams is significantly related to PC3 (Figure 8B, $r = 0.59$, $p < 0.01$), while PC1 variations appear to be associated with current November maximum temperature from Puerto Williams (Figure 8A, $r = 0.46$, $p < 0.01$) and PC2 with prior/current January temperature at 850 mb (Figure 8C, $r = 0.49$, $p < 0.01$). Regarding the atmospheric circulation indices, the most significant relationship was found between PC2 and prior/current summer–fall AAO-Marshall index (Figure 8D, $r = -0.62$, $p < 0.01$).

Our PCs also record the dominant influence of spring–summer and March climate on tree growth at individual sites (Figures 6 and 7), such as the direct relationship of PC3 with wind speed, which is consistent with the strong load of the PYU chronology (located in Yendegaia) in the PC3. In addition, the PCA loadings also reflect the good relation between spring–summer AAO and PC2 at the Navarino Island and Yendegaia sites (NCA, NCB, and YLA).

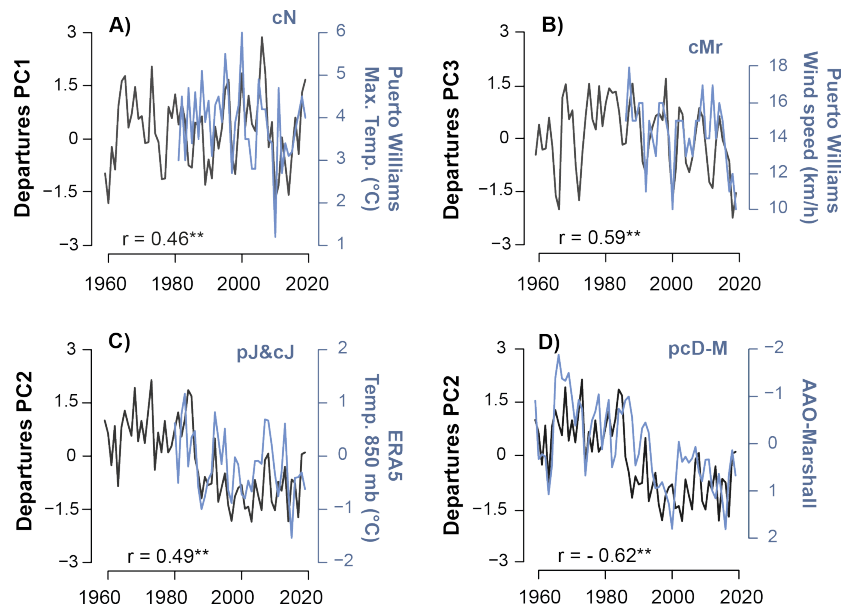


Figure 8. The most significant correlation results for the three PCs departures from SSA with different climate variables (weather stations, ERA5, and AAO index). p -value, **: significant ($p < 0.01$). The best months and combination of months for the climate-tree growth correlations shown here are: (A) cN = current November, (B) cMr = current March, (C) pJ&cJ = previous and current January, and (D) pcD-M = previous and current December to May.

4. Discussion

4.1. Dendrochronological and Dendroclimatic Potential of the Southernmost *Nothofagus* Forests

The *Nothofagus* forests of southernmost South America are the southernmost forest masses of the world [51]. They represent a unique opportunity to study past climate variability in this remote region and document interactions between mid-latitude climatic variations and those of the Antarctic continent. Consistent with previous studies [23,24,26,52,53], the tree-ring chronologies developed in our study show the possibility of obtaining long records, more than 300 years, with an important common signal and highly sensitive to climatic variations. However, these records may reflect the effect of local disturbances that make it difficult to correctly identify the climatic signal present in the tree rings. *Nothofagus* forests in the extreme south of the continent are affected by various disturbances including windthrow, fire, and snow avalanches, among others [51]. Three of our six *N. pumilio* stands (YLA, LTM, and SKI) presented distinctive growth releases potentially attributable to disturbance events during their life cycle. The stands in the northeast of our study area were affected by near-synchronous release events around 1930–1931/1936. A seven-year cycle has been reported in *N. pumilio* forests, most likely associated with cyclic insect attacks [52,54].

In the context of the last 100 years, our tree-ring-based time series (chronologies) reveal anomalous variability of tree growth. The two chronologies of *N. betuloides* from the Navarino Island revealed an exceptional reduction in tree growth since the mid-1980s, with unprecedented levels in at least the last 300 years. These results agree with previous studies, which showed similar reductions in *N. betuloides* chronologies in Navarino Island [23,24]. The recent anomaly in growth reflects to some extent the extreme climatic changes being presently experienced in the extreme south of SA.

By contrast, the radial growth of the *N. pumilio* stands shows greater increments in radial growth in the last decades. Apparent differences between *Nothofagus* stands are probably a combined consequence of a strong regional climatic gradient [29,34], associated with different microsite conditions, water availability [22,25,26,32], and intraspecies and interspecies variations related to genetics (or ontogeny) and different physiological strategies in the face of a water stress period [33,55,56].

4.2. High Diversity of Climatic Responses in SSA *Nothofagus* Forests

The presence of the Andes Mountains introduces marked environmental gradients that result in a great variety in the growth responses of *Nothofagus* forests to climatic variations. Thus, our results and previous studies indicate that *Nothofagus* chronologies in the southernmost part of the continent offer the enormous possibility of reconstructing changes in surface and 850 mb temperature, relative humidity, wind intensity, and their associations with the main atmospheric circulation patterns, including the AAO. Warmer temperatures and reduced precipitation associated with the persistent positive phase of the AAO in spring–summer [28,29] negatively influence the growth of *N. betuloides* forests in Navarino Island. Warmer and drier climatic conditions in recent decades have induced stomatal closure and the consequent decrease in the photosynthetic rate [57,58]. Hence, lower interannual biomass production is reflected in the *N. betuloides* RWIs.

Summer relative humidity is strongly associated with tree growth at SKI in the extreme northeast sector of our study region. Relative humidity, frequently related to soil moisture, modulates the growth of trees in drier environments, especially in the forest-steppe ecotone as documented for North Patagonia [10–12]. The extreme growth reductions (1991/1992, 1999/2000, 2005, 2011/2012) in the SKI chronology were concurrent with low relative humidity during the heatwave and extreme drought events. Mean maximum temperatures in February 1990, 2004, and 2005 (17.3 °C, 17.2 °C, and 17.2 °C, respectively) were the highest since 1930. In addition, an extremely dry (3.2 mm) event was recorded in February 2005, compared to the long-term mean (Supplementary Figure S8) for this month. The summer of 2005 represented an extreme hot-dry event with negative consequences for tree growth at

the SKI site. Hot droughts, a combination of dry days with above-mean temperatures [59] are projected to increase in the future with harmful effects to southern ecosystems [17,60,61].

Although precipitation is not strongly related to tree growth in our study region, significant relationships were documented between spring–summer precipitation and the growth of *Nothofagus* forests at Navarino Island (Supplementary Figures S5 and S6), particularly at sites showing reduced soil depth and steep slopes [26].

4.3. Different Intra- and Inter-Species Sensitivities to Climate

In our study, we recorded marked intra- and inter-species differences in the sensitivity to the climate of the investigated forests. For example, although the *N. pumilio* stands in Punta Arenas (SKI and LTM) are separated by only 40 km, they show differences in tree growth response to climate. The differences in responses can be explained by the drier conditions (470 mm/yr) at the SKI site, where the extreme events (heatwaves and extreme drought) during the summer season (more specifically in February) lead to extreme water deficits limiting tree growth. In comparison, at LTM stands with better soil water conditions (800 mm/yr), spring–summer temperatures are the dominant forcing of tree growth [32,52,53,62]. These marked differences in tree response to climate could also be exacerbated by contrasting disturbance histories between sites. The SKY site is highly disturbed by previous forest fires, logging activities, and the opening of the forest to create space for sky fields.

Contrasting patterns in tree response to climate are also recorded at the *Nothofagus* spp. forests in the Yendegaia Valley and Navarino Island. Different ecophysiological responses to wind between species could explain the recorded patterns. The Navarino Island sites are exposed to constant winds predominantly from the south, creating a constant wind tunnel through the Ukika valley (Figure 1). Such permanent wind stress induce the closure of the trees' stomata to avoid convective forces and hydric deficit [63,64]. In addition, depending on wind speed can cause causes mechanical damage that alters transpiration rates by removing or reducing the superficial leaves layers [63]. In extreme cases of strong winds these can lead to massive leaf death events with an abrupt reduction in tree growth [65]. In contrast, at the Yendegaia sites, although located close to the upper tree-line, the stands are protected from predominant southwesterly winds by surrounding mountains that assumably block or reduce the negative impact of strong winds.

Inter-species differences in tree growth responses to climate were observed at the Navarino island. Both the *N. betuloides* and *N. pumilio* stands, with less than 4 km distance between them, showed contrasting sensitivities to local temperature, precipitation, and atmospheric circulation indices (AAO). The deciduous *Nothofagus* species (including *N. pumilio*) reveal an anisohydric behavior having open stomata even under conditions of marked water stress. As a result, the *N. pumilio* trees are prone to enhanced water loss by constant transpiration [55,66]. Instead, the evergreen species of *Nothofagus*, such as *N. dombeyi*, present a wide variation in their physiological responses to dehydration [56]. The evergreen *N. betuloides* could present some physiological traits that facilitate an adjustment at the level of stomata or photosynthesis and, as a consequence, a reduction in the negative effects of dry-warm climate related to the predominant positive phase of spring–summer AAO in the last decades. However, a combined physiological and morphological approach is needed to fully assess the causes of the different responses of southernmost *Nothofagus* forests to climate variability.

5. Conclusions

We report the findings of the research based on the comparison of eight *Nothofagus* chronologies from southernmost South America (SSA) and their response to climate. We demonstrate a high diversity of climatic responses in *Nothofagus* forests, including new correlations with wind speeds, the temperature at 850 mb, relative humidity, and AAO with potential future reconstruction. *Nothofagus* forests also reveal contrasting climatic responses as a strong climatic gradient effect given by the Andes Mountains, suggest-

ing different strategies due to different microsite conditions and adaptation to drought marked by different sensitivities both at the intra- and inter-species levels in *Nothofagus* stands. Under this evidence, we partially accept our initial hypothesis, given that some *Nothofagus* stands are more sensitive to local climate and other large-scale circulations such as AAO variations. According to recent climate projections, temperature increases, droughts, and extreme events will continue [8]. Hence, we can state that the southernmost *Nothofagus* forests located at the extremes of our study distribution will continue to be subjected to effects derived from local and large-scale climatic variations. Future studies should investigate the physiological strategies of *Nothofagus* spp. and evaluate the risk of crown death and/or mass dieback in the face of an extreme climatic events. The southern *Nothofagus* forests provide critical ecosystem services to the environment, such as carbon sequestration, water regulation, and reduction of natural hazards such as rockslides and snow avalanches. In addition, SSA forests improve water quality and provide recreational sites and firewood for local communities [67–69].

Supplementary Materials: The following supporting information can be downloaded at: <https://www.mdpi.com/article/10.3390/f13050794/s1>, Figure S1: Monthly climate time series from Puerto Williams weather station between January 1968 and December 2020 for (A) temperature (in °C); (B) precipitation (in mm) and (C) wind speed (in km/h); Figure S2: The 3D PCA plot for *Nothofagus* spp. tree growth chronologies. *N. pumilio* and *N. betuloides* chronologies are shown with orange and green colors, respectively; Figure S3: Monthly, season and the best combination of months of Pearson correlation coefficients between Punta Arenas study area tree-ring SKI/LTM chronologies (*N. pumilio*) and climate variables from the weather station, ERA5 data, and AAO indices; Figure S4: Monthly, season and the best combination of months of Pearson correlation coefficients between Yendegaia Valley study area tree-ring YLA/PYU chronologies (*N. pumilio*) and climate variables from the weather station, ERA5 data, and AAO indices; Figure S5: Monthly, season and the best combination of months of Pearson correlation coefficients between Navarino Island (Ukika Valley) study area tree-ring NLN/NLS chronologies (*N. pumilio*) and climate variables from the weather station, ERA5 data, and AAO indices; Figure S6: Monthly, season and the best combination of months of Pearson correlation coefficients between Navarino Island (Ukika Valley) study area tree-ring NCB/NCA chronologies (*N. betuloides*) and climate variables from the weather station, ERA5 data, and AAO indices; Figure S7: Monthly, season and the best combination of months of Pearson correlation coefficients between principal components (PCs) and climate variables from the weather station, ERA5 data, and AAO indices; Figure S8: Time-series: (A) maximum temperature (in °C), (B) precipitation (mm), (C) standardized precipitation- evapotranspiration index (SPEI), (D) relative humidity (%) and (E) SKI tree-ring index of *Nothofagus pumilio*; Table S1: Statistical characteristics of our tree-ring chronologies.

Author Contributions: Conceptualization, P.S.-R., J.C.A. and J.G.; methodology, P.S.-R., J.C.A., C.B., Á.G.-R. and W.J.-H.M.; Formal analysis, P.S.-R.; writing—original draft preparation, P.S.-R. and J.C.A.; writing—review and editing, J.C.A., J.G., W.J.-H.M. and R.V. All authors have read and agreed to the published version of the manuscript.

Funding: This work was supported by the ANID-Chilean scholarship (grant 72190234) and by the ANID-BMBF project AVOID (grant no. 180005 and FKZ 01DN19036). J.C.A. acknowledges Fondecyt (grant 1180717) and ANID/BASAL FB210018.

Data Availability Statement: Our data and results are available to everyone interested in our research.

Acknowledgments: We would like to thank Jorge Arigony for providing the Shiaparelli Glacier weather station data used in Figure 1 and Nicolas Butorovich, Jorge Carrasco, and René Garreaud for explaining the importance of heatwaves and lowest precipitation (drought) in the Magallanes region.

Conflicts of Interest: The authors declare no conflict of interest.

References

- Ciais, P.; Reichstein, M.; Viovy, N.; Granier, A.; Ogee, J.; Allard, V.; Aubinet, M.; Buchmann, N.; Bernhofer, C.; Carrara, A.; et al. Europe-wide reduction in primary productivity caused by the heat and drought in 2003. *Nature* **2005**, *437*, 529–533. [[CrossRef](#)] [[PubMed](#)]
- Allen, C.D.; Macalady, A.K.; Chenchouni, H.; Bachelet, D.; McDowell, N.; Vennetier, M.; Kitzberger, T.; Rigling, A.; Breshears, D.D.; Hogg, E.T.; et al. A global overview of drought and heat-induced tree mortality reveals emerging climate change risks for forests. *For. Ecol. Manag.* **2010**, *259*, 660–684. [[CrossRef](#)]
- Allen, C.D.; Breshears, D.D.; McDowell, N.G. On underestimation of global vulnerability to tree mortality and forest die-off from hotter drought in the Anthropocene. *Ecosphere* **2015**, *6*, 1–55. [[CrossRef](#)]
- Zhao, M.; Running, S.W. Drought-Induced Reduction in Global Terrestrial Net Primary Production from 2000 Through 2009. *Science* **2010**, *329*, 940–943. [[CrossRef](#)]
- Anderegg, W.R.L.; Schwalm, C.; Biondi, F.; Camarero, J.J.; Koch, G.; Litvak, M.; Ogle, K.; Shaw, J.D.; Shevliakova, E.; Williams, A.P.; et al. Pervasive drought legacies in forest ecosystems and their implications for carbon cycle models. *Science* **2015**, *349*, 528–532. [[CrossRef](#)]
- McDowell, N.G.; Allen, C.D.; Anderson-Teixeira, K.; Aukema, B.H.; Bond-Lamberty, B.; Chini, L.; Clark, J.S.; Dietze, M.; Grossiord, C.; Hanbury-Brown, A.; et al. Pervasive shifts in forest dynamics in a changing world. *Science* **2020**, *368*, eaaz9463. [[CrossRef](#)]
- Büntgen, U.; Urban, O.; Krusic, P.J.; Rybníček, M.; Kolář, T.; Kyncl, T.; Ač, A.; Koňasová, E.; Čáslavský, J.; Esper, J.; et al. Recent European drought extremes beyond Common Era background variability. *Nat. Geosci.* **2021**, *14*, 190–196. [[CrossRef](#)]
- Arias, P.; Bellouin, N.; Coppola, E.; Jones, R.; Krinner, G.; Marotzke, J.; Naik, V.; Palmer, M.; Plattner, G.K.; Rogelj, J.; et al. Technical Summary. In *Climate Change 2021: The Physical Science Basis. Contribution of Working Group I to the Sixth Assessment Report of the Intergovernmental Panel on Climate Change*; Masson-Delmotte, V., Zhai, P., Pirani, A., Connors, S.L., Péan, C., Berger, S., Caud, N., Chen, Y., Goldfarb, L., Gomis, M.I., et al., Eds.; Cambridge University Press: Cambridge, UK; New York, NY, USA, 2021; pp. 33–144.
- Bréda, N.; Huc, R.; Granier, A.; Dreyer, E. Temperate forest trees and stands under severe drought: A review of ecophysiological responses, adaptation processes and long-term consequences. *Ann. For. Sci.* **2006**, *63*, 625–644. [[CrossRef](#)]
- Villalba, R.; Veblen, T.T. Influences of Large-Scale Climatic Variability on Episodic Tree Mortality in Northern Patagonia. *Ecology* **1998**, *79*, 2624. [[CrossRef](#)]
- Suarez, M.L.; Ghermandi, L.; Kitzberger, T. Factors predisposing episodic drought-induced tree mortality in *Nothofagus*—Site, climatic sensitivity and growth trends. *J. Ecol.* **2004**, *92*, 954–966. [[CrossRef](#)]
- Mundo, I.A.; Mujtar, V.A.E.; Perdomo, M.H.; Gallo, L.A.; Villalba, R.; Barrera, M.D. *Austrocedrus chilensis* growth decline in relation to drought events in northern Patagonia, Argentina. *Trees* **2010**, *24*, 561–570. [[CrossRef](#)]
- Rodríguez-Catón, M.; Villalba, R.; Srur, A.M.; Luckman, B. Long-term trends in radial growth associated with *Nothofagus pumilio* forest decline in Patagonia: Integrating local- into regional-scale patterns. *For. Ecol. Manag.* **2015**, *339*, 44–56. [[CrossRef](#)]
- Rodríguez-Catón, M.; Villalba, R.; Morales, M.; Srur, A. Influence of droughts on *Nothofagus pumilio* forest decline across northern Patagonia, Argentina. *Ecosphere* **2016**, *7*, e01390. [[CrossRef](#)]
- Tarabini, M.; Gomez, F.; Ángel Calderón, M.; Manna, L.L. Role of abiotic factors in *Nothofagus pumilio* forest mortality: The sensitivity of ecotones. *For. Ecol. Manag.* **2021**, *494*, 119316. [[CrossRef](#)]
- Urrutia-Jalabert, R.; Barichivich, J.; Rozas, V.; Lara, A.; Rojas, Y.; Bahamondez, C.; Rojas-Badilla, M.; Gipoulou-Zuñiga, T.; Cuq, E. Climate response and drought resilience of *Nothofagus obliqua* secondary forests across a latitudinal gradient in south-central Chile. *For. Ecol. Manag.* **2021**, *485*, 118962. [[CrossRef](#)]
- Puchi, P.F.; Camarero, J.J.; Battipaglia, G.; Carrer, M. Retrospective analysis of wood anatomical traits and tree-ring isotopes suggests site-specific mechanisms triggering *Araucaria araucana* drought-induced dieback. *Glob. Chang. Biol.* **2021**, *27*, 6394–6408. [[CrossRef](#)]
- Urrutia-Jalabert, R.; Malhi, Y.; Barichivich, J.; Lara, A.; Delgado-Huertas, A.; Rodríguez, C.G.; Cuq, E. Increased water use efficiency but contrasting tree growth patterns in *Fitzroya cupressoides* forests of southern Chile during recent decades. *J. Geophys. Res. Biogeosci.* **2015**, *120*, 2505–2524. [[CrossRef](#)]
- Lavergne, A.; Daux, V.; Villalba, R.; Pierre, M.; Stievenard, M.; Srur, A.M. Improvement of isotope-based climate reconstructions in Patagonia through a better understanding of climate influences on isotopic fractionation in tree rings. *Earth Planet. Sci. Lett.* **2017**, *459*, 372–380. [[CrossRef](#)]
- Pisano, E. Fitogeografía de Fuego-Patagonia chilena I- Comunidades vegetales entre las latitudes 52 y 56 s. *An. Inst. Patagon.* **1977**, *8*, 121–250.
- Donoso, C. *Tipos Forestales de los Bosques Nativos de Chile*; Santiago, Chile, 1981; p. 70. Available online: <https://bibliotecadigital.infor.cl/handle/20.500.12220/6178> (accessed on 1 March 2022).
- Srur, A.M.; Villalba, R.; Villagra, P.E.; Hertel, D. Influencias de las variaciones en el clima y en la concentración de CO₂ sobre el crecimiento de *Nothofagus pumilio* en la Patagon. *Rev. Chil. Hist. Nat.* **2008**, *81*, 239–256. [[CrossRef](#)]
- Llancabure, J.C. Relaciones entre el crecimiento de *Nothofagus Betuloides* y el Clima Local y de Gran Escala en Bosques Subantárticos de la Isla Navarino. Bachelor's Thesis, Universidad Austral de Chile, Valdivia, Chile, 2011.

24. Villalba, R.; Lara, A.; Masiokas, M.; Urrutia, R.; Luckman, B.H.; Marshall, G.J.; Mundo, I.A.; Christie, D.A.; Cook, E.R.; Neukom, R.; et al. Unusual Southern Hemisphere tree growth patterns induced by changes in the Southern Annular Mode. *Nat. Geosci.* **2012**, *5*, 793–798. [[CrossRef](#)]
25. Soto-Rogel, P.; Aravena, J. Potencial dendroclimático de *Nothofagus betuloides* en la cordillera de Darwin, Tierra del Fuego, Chile. *Bosque* **2017**, *38*, 155–168. [[CrossRef](#)]
26. Fuentes, M.; Aravena, J.C.; Seim, A.; Linderholm, H.W. Assessing the dendroclimatic potential of *Nothofagus betuloides* (Magellan's beech) forests in the southernmost Chilean Patagonia. *Trees* **2019**, *33*, 557–575. [[CrossRef](#)]
27. Marshall, G.J. Trends in the Southern Annular Mode from observations and reanalyses. *J. Clim.* **2003**, *16*, 4134–4143. [[CrossRef](#)]
28. Carrasco, J.F. Decadal Changes in the Near-Surface Air Temperature in the Western Side of the Antarctic Peninsula. *Atmos. Clim. Sci.* **2013**, *3*, 33653. [[CrossRef](#)]
29. González-Reyes, Á.; Aravena, J.C.; Muñoz, A.A.; Soto-Rogel, P.; Aguilera-Betti, I.; Toledo-Guerrero, I. Variabilidad de la precipitación en la ciudad de Punta Arenas, Chile, desde principios del siglo XX. *An. Inst. Patagon.* **2017**, *45*, 31–44. [[CrossRef](#)]
30. Soto-Rogel, P.; Aravena, J.C.; Meier, W.J.H.; Gross, P.; Pérez, C.; González-Reyes, Á.; Griessinger, J. Impact of Extreme Weather Events on Aboveground Net Primary Productivity and Sheep Production in the Magellan Region, Southernmost Chilean Patagonia. *Geosciences* **2020**, *10*, 318. [[CrossRef](#)]
31. Dirección Meteorológica de Chile. Available online: <http://www.meteochile.gob.cl/PortalDMC-web/index.xhtml> (accessed on 1 May 2022).
32. Massaccesi, G.; Roig, F.A.; Martínez Pastur, G.J.; Barrera, M.D. Growth patterns of *Nothofagus pumilio* trees along altitudinal gradients in Tierra del Fuego, Argentina. *Trees* **2008**, *22*, 245–255. [[CrossRef](#)]
33. Soliani, C.; Mattera, M.G.; Marchelli, P.; Azpilicueta, M.M.; Dalla-Salda, G. Different drought-adaptive capacity of a native Patagonian tree species (*Nothofagus pumilio*) resulting from local adaptation. *Eur. J. For. Res.* **2021**, *140*, 1147–1161. [[CrossRef](#)]
34. Carrasco, J.F.; Casassa, G.; Rivera, A. Meteorological and Climatological Aspects of the Southern Patagonia Icefield. In *The Patagonian Icefields: A Unique Natural Laboratory for Environmental and Climate Change Studies*; Casassa, G., Sepúlveda, F.V., Sinclair, R.M., Eds.; Springer: Boston, MA, USA, 2002; pp. 29–41. [[CrossRef](#)]
35. Luebert, F.; Plischoff, P. *Sinopsis Bioclimática y Vegetacional de Chile*; Editorial Universitaria: Santiago, Chile, 1977; p. 384.
36. Stokes, M.A.; Smiley, T.L. *An Introduction to Tree-Ring Dating*; University of Arizona Press: Tucson AZ, USA, 1996; p. 73.
37. Schulman, E. *Dendroclimatic Changes in Semiarid America*; University of Arizona Press: Tucson, AZ, USA, 1956; p. 142.
38. Robinson, W.J.; Evans, R. A Microcomputer-Based Tree-Ring Measuring System. *Tree-Ring Bull.* **1980**, *40*, 59–64.
39. Holmes, R.L. Computer-Assisted Quality Control in Tree-Ring Dating and Measurement. *Tree-Ring Bull.* **1983**, *43*, 51–67.
40. Bunn, A.G. A dendrochronology program library in R (dplR). *Dendrochronologia* **2008**, *26*, 115–124. [[CrossRef](#)]
41. R Core Team. *R: A Language and Environment for Statistical Computing*; R Foundation for Statistical Computing: Vienna, Austria, 2021.
42. Fritts, H.C. *Tree Rings and Climate*; Academic Press: London, UK, 1976; p. 567.
43. Briffa, K.; Jones, P., Basic chronology statistics and assessment. In *Methods of Dendrochronology: Applications in the Environmental Sciences*; Cook, E., Kairiukstis, L., Eds.; Kluwer Academic Publishers: Dordrecht, The Netherlands, 1990; pp. 137–152.
44. Cook, E.R.; Briffa, K.R.; Jones, P.D. Spatial Regression Methods in Dendroclimatology: A review and comparison of two techniques. *Int. J. Climatol.* **1994**, *14*, 379–402. [[CrossRef](#)]
45. Wilks, D.S. *Statistical Methods in the Atmospheric Sciences*; Elsevier Academic Press: Amsterdam, The Netherlands; Boston, MA, USA, 2011.
46. Revelle, W. *psych: Procedures for Psychological, Psychometric, and Personality Research*; R Package Version 2.1.9; Northwestern University: Evanston, IL, USA, 2021.
47. Rodionov, S.N. A sequential algorithm for testing climate regime shifts. *Geophys. Res. Lett.* **2004**, *31*. [[CrossRef](#)]
48. Hersbach, H.; Bell, B.; Berrisford, P.; Hirahara, S.; Horányi, A.; Muñoz-Sabater, J.; Nicolas, J.P.; Peubey, C.; Radu, R.; Schepers, D.; et al. The ERA5 global reanalysis. *Q. J. R. Meteorol. Soc.* **2020**, *146*, 1999–2049. [[CrossRef](#)]
49. Climate Prediction Center. Available online: https://www.cpc.ncep.noaa.gov/products/precip/CWlink/daily_ao_index/aao/aao.shtml (accessed on 1 May 2022).
50. Wigley, T.M.L.; Briffa, K.R.; Jones, P.D. On the Average Value of Correlated Time Series, with Applications in Dendroclimatology and Hydrometeorology. *J. Appl. Meteorol. Climatol.* **1984**, *23*, 201–213. [[CrossRef](#)]
51. Veblen, T.T.; Kitzberger, T.; Donoso, C.; Rebertus, A.J., Ecology of southern Chilean and Argentinean *Nothofagus* forests. In *The Ecology and Biogeography of Nothofagus Forests*; Veblen, T.T., Hill, R.S., Read, J., Eds.; Yale University Press: New Haven, CT, USA, 1996; p. 403.
52. Aravena, J.C.; Lara, A.; Wlodarsky-Franke, E.; Villalba, R.; Cuq, E. Tree-ring growth patterns and temperature reconstruction from *Nothofagus pumilio* (Fagaceae) forests at the upper tree line of southern Chilean Patagonia. *Rev. Chil. Hist. Nat.* **2002**, *75*, 361–376. [[CrossRef](#)]
53. Villalba, R.; Lara, A.; Boninsegna, J.A.; Masiokas, M.; Delgado, S.; Aravena, J.C.; Roig, F.A.; Schmelter, A.; Wolodarsky, A.; Ripalta, A. Large-scale temperature changes across the Southern Andes: 20th-century variations in the context of the past 400 years. *Clim. Chang.* **2003**, *59*, 177–232. [[CrossRef](#)]

54. Matskovsky, V.; Roig, F.A.; Martínez Pastur, G. Removal of a non-climatically induced seven-year cycle from *Nothofagus pumilio* tree-ring width chronologies from Tierra del Fuego, Argentina for their use in climate reconstructions. *Dendrochronologia* **2019**, *57*, 125610. [[CrossRef](#)]
55. Varela, S.A.; Gyenge, J.E.; Fernández, M.E.; Schlichter, T. Seedling drought stress susceptibility in two deciduous *Nothofagus* species of NW Patagonia. *Trees* **2010**, *24*, 443–453. [[CrossRef](#)]
56. Bucci, S.J.; Silletta, L.M.C.; Garré, A.; Cavallaro, A.; Efron, S.T.; Arias, N.S.; Goldstein, G.; Scholz, F.G. Functional relationships between hydraulic traits and the timing of diurnal depression of photosynthesis. *Plant Cell Environ.* **2019**, *42*, 1603–1614. [[CrossRef](#)] [[PubMed](#)]
57. Meier, W.H.; Aravena, J.C.; Jaña, R.; Braun, M.; Hochreuther, P.; Soto-Rogel, P.; Griesinger, J. A tree-ring d18O series from southernmost Fuego-Patagonia is recording flavors of the Antarctic Oscillation. *Glob. Planet. Chang.* **2020**, *195*, 103302. [[CrossRef](#)]
58. Han, Y.; Wang, Y.; Liu, B.; Huang, R.; Camarero, J.J. Moisture mediates temperature-growth couplings of high-elevation shrubs in the Tibetan plateau. *Trees* **2022**, *36*, 273–281. [[CrossRef](#)]
59. Mueller, B.; Seneviratne, S.I. Hot days induced by precipitation deficits at the global scale. *Proc. Natl. Acad. Sci. USA* **2012**, *109*, 12398–12403. [[CrossRef](#)] [[PubMed](#)]
60. Williams, A.P.; Allen, C.D.; Macalady, A.K.; Griffin, D.; Woodhouse, C.A.; Meko, D.M.; Swetnam, T.W.; Rauscher, S.A.; Seager, R.; Grissino-Mayer, H.D.; et al. Temperature as a potent driver of regional forest drought stress and tree mortality. *Nat. Clim. Change* **2013**, *3*, 292–297. [[CrossRef](#)]
61. Gazol, A.; Camarero, J.J. Compound climate events increase tree drought mortality across European forests. *Sci. Total Environ.* **2021**, *816*, 151604. [[CrossRef](#)]
62. Boninsegna, J.A.; Keegan, J.; Jacoby, G.C.; D'Arrigo, R.; Holmes, R.L. Dendrochronological studies in Tierra del Fuego, Argentina. In *Quaternary of South America and Antarctic Peninsula*; Rabassa, J., Ed.; CRC Press: Boca Raton, FL, USA, 1989; pp. 305–326.
63. Smith, V.C.; Ennos, A.R. The effects of air flow and stem flexure on the mechanical and hydraulic properties of the stems of sunflowers *Helianthus annuus* L. *J. Exp. Bot.* **2003**, *54*, 845–849. [[CrossRef](#)]
64. Iogna, P.A.; Bucci, S.J.; Scholz, F.G.; Goldstein, G. Homeostasis in leaf water potentials on leeward and windward sides of desert shrub crowns: Water loss control vs. high hydraulic efficiency. *Oecologia* **2013**, *173*, 675–687. [[CrossRef](#)]
65. Seo, J.W.; Choi, E.B.; Park, J.H.; Kim, Y.J.; Lim, H.I. The Role of Aging and Wind in Inducing Death and/or Growth Reduction in Korean Fir (*Abies Koreana* Wilson) on Mt. Halla, Korea. *Atmosphere* **2021**, *12*, 1135. [[CrossRef](#)]
66. Bahamonde, H.A.; Sánchez-Gómez, D.; Gyenge, J.; Peri, P.L.; Cellini, J.M.; Aranda, I. Thinking in the sustainability of *Nothofagus antarctica* silvopastoral systems, how differ the responses of seedlings from different provenances to water shortage? *Agrofor. Syst.* **2019**, *93*, 689–701. [[CrossRef](#)]
67. Oyarzún, C.; Nahuelhual, L.; Núñez, D. Los servicios ecosistémicos del bosque templado lluvioso: Producción de agua y su valoración económica. *Rev. Ambi. Desarro.* **2005**, *20*, 88–95.
68. Jobbágy, E.G. Servicios hídricos de los ecosistemas y su relación con el uso de la tierra en la llanura Chaco-Pampeana. In *Valoración de Servicios Ecosistémicos Conceptos, Herramientas y Aplicaciones para el Ordenamiento Territorial*; Littera, P., Jobbágy, E.G., Paruelo, J., Eds.; Ediciones INTA: New York, NY, USA, 2011; pp. 163–183.
69. Hoyos-Santillan, J.; Miranda, A.; Lara, A.; Sepulveda-Jauregui, A.; Zamorano-Elgueta, C.; Gómez-González, S.; Vásquez-Lavín, F.; Garreaud, R.D.; Rojas, M. Diversifying Chile's climate action away from industrial plantations. *Environ. Sci. Policy* **2021**, *124*, 85–89. [[CrossRef](#)]